

## Supporting Information

### Surface Phosphorization of NiCo<sub>2</sub>S<sub>4</sub> as Efficient Bifunctional Electrocatalyst for Full Water Splitting

Hua Yang, Kangdi Lin, Zihao Zhou, Chenting Peng, Shaomin Peng\*, Ming Sun\*, Lin Yu

Key Laboratory of Clean Chemistry Technology of Guangdong Regular Higher Education  
Institutions, Guangdong Provincial Key Laboratory of Plant Resources Biorefinery, School of  
Chemical Engineering and Light Industry, Guangdong University of Technology, 510006  
Guangzhou, P. R. China

\*Corresponding author: smpeng0814@gdut.edu.cn; sunmgz@gdut.edu.cn

## 1. Characterization details

X-ray diffraction test (XRD) was performed on a PANalytical X-ray Diffractometer (Aeris) equipped with a Cu K $\alpha$  radiation. The field emission scanning electron microscope (FE-SEM) images were obtained on a Hitachi SU8220 instrument. Transmission electron microscopy (TEM) images and energy-dispersive spectrometer elemental mapping (EDS-mapping) were acquired on a FEI Talos F200S with an accelerating voltage of 200 kV. X-ray photoelectron spectroscopy (XPS) was test on a Thermo Fisher Escalab 250Xi spectrometer. The XPS in-depth test uses a 3 keV Ar ion gun for sputtering, the sputtering area is 1mm\*1mm, the sputtering rate is calibrated by thermally oxidized SiO<sub>2</sub> (standard sample) to 25 nm/min, and each sputtering time is 120 s (for 50 nm). The total etching depth is 200 nm.

## 2. Electrochemical measurements

The electrochemical experiments were carried out on an electrochemical workstation (German, ZAHNER ZENNIUM) using a standard three-electrode system. The Ni-Co-S-P/CFP with area of 1 cm<sup>2</sup> served as the working electrode, and graphite rod and Pt foil served as counter electrodes for HER and OER, respectively. The Ag/AgCl (3.5 M KCl, 0.2046 V vs. RHE) electrode was used as a reference electrode in alkaline media (1.0 M KOH, pH $\approx$ 14). The measured potentials were converted to the reversible hydrogen electrode (RHE) using the following equation:  $E_{RHE} = E_{Hg/HgO} + 0.059pH + E_{Hg/HgO}^0$  and  $E_{RHE} = E_{SCE} + 0.059pH + E_{SCE}^0$ , and all potentials were not iR-corrected to avoid the effects of large differences in iR compensation. All electrochemical tests were first activated by continuous cyclic voltammetry (CV), and the linear sweep voltammetry (LSV) tests were at a slow scan rate of 1 mV s<sup>-1</sup>. Electrochemical impedance spectroscopy (EIS) measurement was carried out at different overpotentials in the frequency range of 10 kHz to 10 mHz with a 5 mV ac amplitude. According to Polarization curves, the Tafel plots were plotted by fitting to the Tafel equation:  $\eta = a + b \log j$  (where  $\eta$  is the overpotential,  $a$  is the intercept relative to the exchange current density ( $j_0$ ),  $j$  is the current density and  $b$  is the Tafel slope). The long-term stability was tested by a galvanostatic method at current density of 10 mA cm<sup>-2</sup> (in 1 M KOH). The electrochemical active surface areas (ECSA) of catalysts were estimated by the double layer capacitance ( $C_{dl}$ ), which is linearly proportional to the ECSA. The

$C_{dl}$  was determined by using the cyclic voltammograms (CVs) recorded at non-Faradaic potentials (0.43-0.59 V vs. RHE for HER) at different scan rates.

The overall water-splitting test was performed in a two-electrode system by directly using Ni-Co-S-P/CFP as both the cathode and anode. The LSV curves were recorded in 1.0 M KOH with a scan rate of  $1 \text{ mV s}^{-1}$ . The long-term durability was tested by the galvanostatic method.

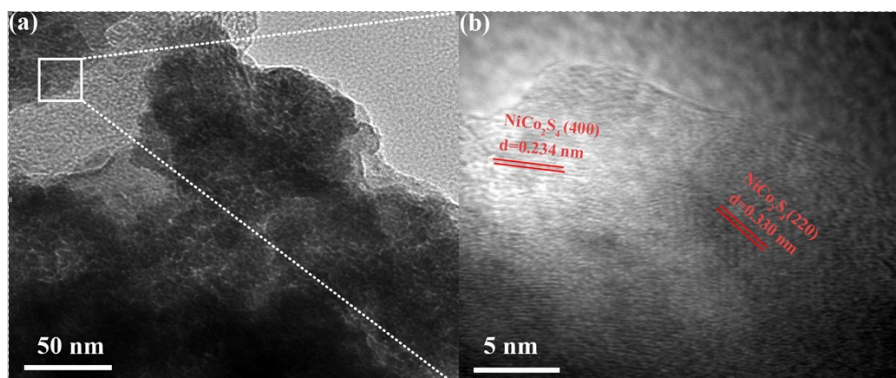


Fig. S1 HRTEM images of Ni-Co-S

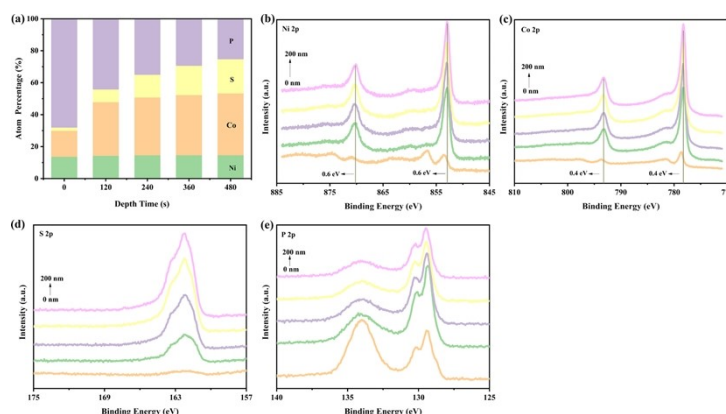


Fig.S2 XPS in-depth analysis using Ar ion etching

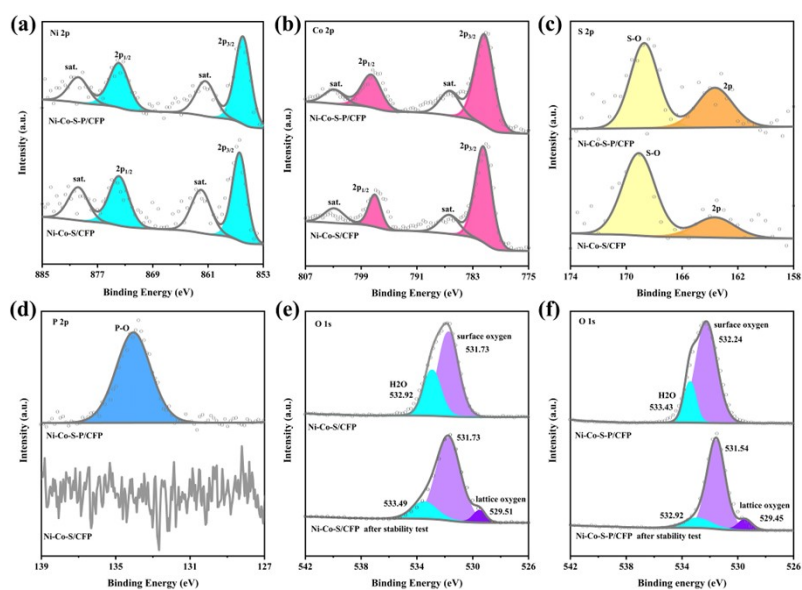


Fig.S3 High-resolution XPS spectra after stability test: (a) Ni 2p, (b) Co 2p, (c) S 2p, (d) P 2p, O 1s spectra of (e) Ni-Co-S/CFP and (f) Ni-Co-S-P/CFP .

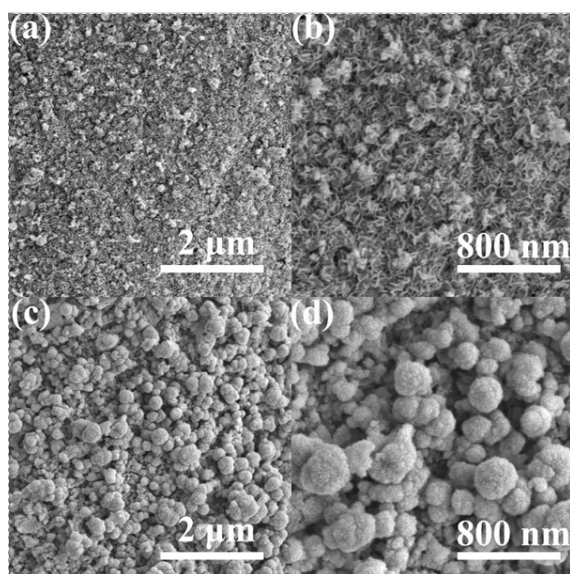


Fig. S4 SEM images of Ni-Co-S-P/CFP after (a,b) HER, (c,d) OER stability test.

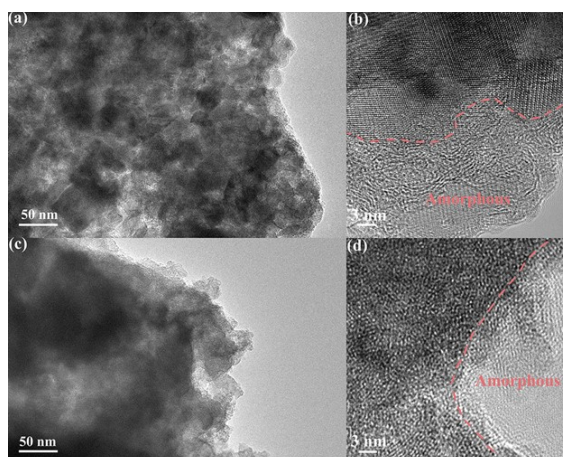


Fig. S5 HRTEM images of Ni-Co-S-P/CFP after (a,b) HER, (c,d) OER stability test.

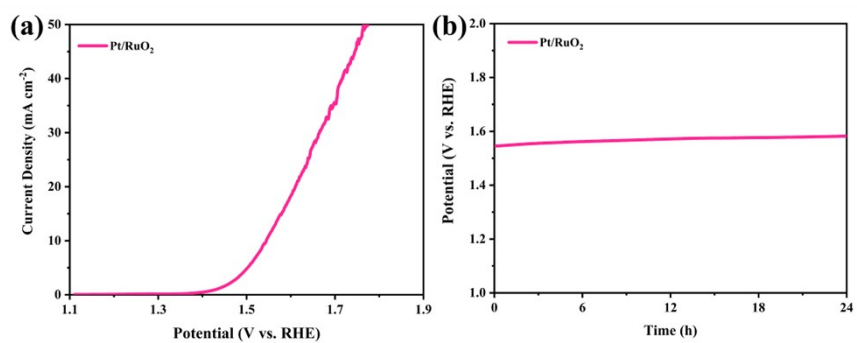


Fig.S6 (a) Polarization curve of overall water-splitting using Pt/RuO<sub>2</sub> as both anode and cathode electrocatalysts in a two-electrode system.

(b) Long-term stability at 10 mA cm<sup>-2</sup> .

**Table S1. Comparison of OER activity of various TMPs based catalysts.**

<b>electrocatalysts</b>	<b>Media</b>	<b><math>\eta_{10}</math> /m V</b>	<b><math>\eta_{100}</math> /m V</b>	<b>Reference</b>
Ni-Co-S-P/CFP	1 M KOH	265	413	This Work
Co-P	1 M KOH	345		[1]
Ni <sub>3</sub> S <sub>2</sub> /NF	1 M KOH	312	467	[2]
Ni-Co-S-P	1 M KOH	280		[3]
CoP/NCNHP	1 M KOH	310		[4]
NiCo/NiCoO@FeOO H	1 M KOH	278		[5]
Co <sub>9</sub> S <sub>8</sub>	1 M KOH	299	430	[6]
NiCo/CNF@NC	1 M KOH	350		[7]
NiCo <sub>2</sub> O <sub>4</sub> /CN	1 M KOH	383		[8]
Ni-Co-Fe (NCF)- MOF	0.1 M KOH	320		[9]
P,S-CoxOy /Cu@CuS NWs	1 M KOH	280		[10]
Co <sub>2</sub> B/NG	0.1 M KOH	380		[11]
FeCoNi-2	1 M KOH	288		[12]
NiFe LDH/NGF	0.1 M KOH	340		[13]

**Table S2. Comparison of HER activity of various TMPs based catalysts.**

<b>electrocatalysts</b>	<b>Media</b>	<b><math>\eta_{10}</math> /m V</b>	<b><math>\eta_{100}</math> /m V</b>	<b>Reference</b>
Ni-Co-S-P/CFP	1 M KOH	176	342	This Work
Cu <sub>0.3</sub> Co <sub>2.7</sub> P/NC	1 M KOH	220		[14]
Co <sub>9</sub> S <sub>8</sub>	1 M KOH	217		[6]
NiCoS/C	1 M KOH	232		[15]
NiCo/CNF@NC	1 M KOH	220		[7]
Ni-Co-Fe-MOF	0.1 M KOH	270		[9]
NiCo <sub>2</sub> S <sub>4</sub> /NF	1 M KOH	220		[16]
NiCoP/CNTs	1 M KOH	267		[17]
NGO/Ni <sub>7</sub> S <sub>6</sub>	1 M KOH	370		[18]
NiCoP	0.5 M H <sub>2</sub> SO <sub>4</sub>	230		[19]
CoO @CN	1 M KOH	232		[20]
Ni-Co <sub>2</sub> P/NCNTs	0.5 M H <sub>2</sub> SO <sub>4</sub>	230	278 ( $\eta_{20}$ )	[21]
CoMoP	0.5 M H <sub>2</sub> SO <sub>4</sub>	215		[22]
Cu-MoS <sub>2</sub> /rGO	0.5 M H <sub>2</sub> SO <sub>4</sub>		400 ( $\eta_{83.6}$ )	[23]
Co <sub>2</sub> B/NG	1 M KOH	230		[11]

## Reference

- [1] N. Jiang, B. You, M. Sheng, Y. Sun, Electrodeposited cobalt-phosphorous-derived films as competent bifunctional catalysts for overall water splitting, *Angew Chem Int Ed*, 54 (2015) 6251-6254.
- [2] G. Ren, Q. Hao, J. Mao, L. Liang, H. Liu, C. Liu, J. Zhang, Ultrafast fabrication of nickel sulfide film on Ni foam for efficient overall water splitting, *Nanoscale*, 10 (2018) 17347-17353.
- [3] Y. Tian, Z. Lin, J. Yu, S. Zhao, Q. Liu, J. Liu, R. Chen, Y. Qi, H. Zhang, R. Li, J. Li, J. Wang, Superaerophobic Quaternary Ni-Co-S-P Nanoparticles for Efficient Overall Water-Splitting, *ACS Sustainable Chem Eng*, 7 (2019) 14639-14646.
- [4] Y. Pan, K. Sun, S. Liu, X. Cao, K. Wu, W.C. Cheong, Z. Chen, Y. Wang, Y. Li, Y. Liu, D. Wang, Q. Peng, C. Chen, Y. Li, Core-Shell ZIF-8@ZIF-67-Derived CoP Nanoparticle-Embedded N-Doped Carbon Nanotube Hollow Polyhedron for Efficient Overall Water Splitting, *J Am Chem Soc*, 140 (2018) 2610-2618.
- [5] S. Yubo, Z. Meiyong, C. Minmin, H. Lan, X. Cailing, Improved Electrocatalytic Performance of Core-shell NiCo/NiCoO<sub>x</sub> with amorphous FeOOH for Oxygen-evolution Reaction, *Electrochim. Acta*, 257(2017)1-8.
- [6] C. Zhang, S. Bhojate, P.K. Kahol, K. Siam, T.P. Poudel, S.R. Mishra, F. Perez, A. Gupta, G. Gupta, R.K. Gupta, Highly Efficient and Durable Electrocatalyst Based on Nanowires of Cobalt Sulfide for Overall Water Splitting, *ChemNanoMat*, 4 (2018) 1240-1246.
- [7] G. Tesfaye Tadesse, C. Fuyi, J. Yachao, W. Qiao, W. Jiali, W. Junpeng, Bimetallic NiCo/CNF encapsulated in a N-doped carbon shell as an electrocatalyst for Zn-air batteries and water splitting, *Catal Sci Technol*, 9(2019) 2532-2542.
- [8] Y. Li, Z. Zhou, G. Cheng, S. Han, J. Zhou, J. Yuan, M. Sun, L. Yu, Flower-like NiCo<sub>2</sub>O<sub>4</sub>-CN as efficient bifunctional electrocatalyst for Zn-Air battery, *Electrochim Acta*, 341 (2020)135997.
- [9] W. Ahn, M.G. Park, D.U. Lee, M.H. Seo, G. Jiang, Z.P. Cano, F.M. Hassan, Z. Chen, Hollow Multivoid Nanocuboids Derived from Ternary Ni-Co-Fe Prussian Blue Analog for Dual-Electrocatalysis of Oxygen and Hydrogen Evolution Reactions, *Adv Funct Mater*, 28 (2018) 1802129.
- [10] T.L.L. Doan, D.T. Tran, D.C. Nguyen, D.H. Kim, N.H. Kim, J.H. Lee, Rational Engineering Co<sub>x</sub>O<sub>y</sub> Nanosheets via Phosphorous and Sulfur Dual-Coupling for Enhancing Water Splitting and Zn-Air Battery, *Adv Funct Mater*, 31(2020)2007822.
- [11] J. Masa, P. Weide, D. Peeters, I. Sinev, W. Xia, Z. Sun, C. Somsen, M. Muhler, W. Schuhmann, Amorphous Cobalt Boride (Co<sub>2</sub>B) as a Highly Efficient Nonprecious Catalyst for Electrochemical Water Splitting: Oxygen and Hydrogen Evolution, *Adv Funct Mater*, 6 (2016)1502313.
- [12] Y. Yang, Z. Lin, S. Gao, J. Su, Z. Lun, G. Xia, J. Chen, R. Zhang, Q. Chen, Tuning Electronic Structures of Nonprecious Ternary Alloys Encapsulated in Graphene Layers for Optimizing Overall Water Splitting Activity, *ACS Catal*, 7 (2016) 469-479.
- [13] C. Tang, H.S. Wang, H.F. Wang, Q. Zhang, G.L. Tian, J.Q. Nie, F. Wei, Spatially Confined Hybridization of Nanometer-Sized NiFe Hydroxides into Nitrogen-Doped Graphene Frameworks Leading to Superior Oxygen Evolution Reactivity, *Adv Mater*, 27 (2015) 4516-4522.
- [14] J. Song, C. Zhu, B.Z. Xu, S. Fu, M.H. Engelhard, R. Ye, D. Du, S.P. Beckman, Y. Lin, Bimetallic Cobalt-Based Phosphide Zeolitic Imidazolate Framework: CoPxPhase-Dependent Electrical Conductivity and Hydrogen Atom Adsorption Energy for Efficient Overall Water Splitting, *Adv Funct Mater*, 7 (2017)1601555.



- [15] A. Yousuf, N. Van-Toan, N. Ngoc-Anh, S. Sangho, C. Ho-Suk, Transition-metal-based NiCoS/C-dot nanoflower as a stable electrocatalyst for hydrogen evolution reaction, *Int J Hydrogen Energy*, 44(2019) 8214-8222.
- [16] A. Sivanantham, P. Ganesan, S. Shanmugam, Hierarchical NiCo<sub>2</sub>S<sub>4</sub> Nanowire Arrays Supported on Ni Foam: An Efficient and Durable Bifunctional Electrocatalyst for Oxygen and Hydrogen Evolution Reactions, *Adv Funct Mater*, 26 (2016) 4661-4672.
- [17] Q. Wang, M. Hou, Y. Huang, J. Li, X. Zhou, G. Ma, S. Ren, One-pot synthesis of NiCoP/CNTs composites for lithium ion batteries and hydrogen evolution reaction, *Ionics*, 26 (2019) 1771-1778.
- [18] K. Jayaramulu, J. Masa, O. Tomanec, D. Peeters, V. Ranc, A. Schneemann, R. Zboril, W. Schuhmann, R.A. Fischer, Nanoporous Nitrogen-Doped Graphene Oxide/Nickel Sulfide Composite Sheets Derived from a Metal-Organic Framework as an Efficient Electrocatalyst for Hydrogen and Oxygen Evolution, *Adv Funct Mater*, 27 (2017)1700451.
- [19] J. Zhang, L. Zhang, X. Wang, W. Zhu, Z. Zhuang, A hierarchical hollow-on-hollow NiCoP electrocatalyst for efficient hydrogen evolution reaction, *Chem Commun*, 56 (2019) 90-93.
- [20] H. Jin, J. Wang, D. Su, Z. Wei, Z. Pang, Y. Wang, In situ cobalt-cobalt oxide/N-doped carbon hybrids as superior bifunctional electrocatalysts for hydrogen and oxygen evolution, *J Am Chem Soc*, 137 (2015) 2688-2694.
- [21] Y. Pan, Y. Liu, Y. Lin, C. Liu, Metal Doping Effect of the M-Co<sub>2</sub>P/Nitrogen-Doped Carbon Nanotubes (M = Fe, Ni, Cu) Hydrogen Evolution Hybrid Catalysts, *ACS Appl Mater Interfaces*, 8 (2016) 13890-13901.
- [22] D. Wang, X. Zhang, D. Zhang, Y. Shen, Z. Wu, Influence of Mo/P Ratio on CoMoP nanoparticles as highly efficient HER catalysts, *Appl Catal A*, 511 (2016) 11-15.
- [23] F. Li, L. Zhang, J. Li, X. Lin, X. Li, Y. Fang, J. Huang, W. Li, M. Tian, J. Jin, R. Li, Synthesis of Cu-MoS<sub>2</sub>/rGO hybrid as non-noble metal electrocatalysts for the hydrogen evolution reaction, *J Power Sources*, 292 (2015) 15-22.